Global Change Biology (2009) **15**, 1040–1056, doi: 10.1111/j.1365-2486.2008.01773.x

Effect of eutrophication on air–sea CO_2 fluxes in the coastal Southern North Sea: a model study of the past 50 years

N. GYPENS*, A. V. BORGES† and C. LANCELOT*

*Ecologie des Systèmes Aquatiques, Université Libre de Bruxelles, CP 221, Bd du Triomphe, B-1050 Bruxelles, Belgium, †Unité d'Océanographie Chimique, Institut de Physique (B5), Université de Liège, MARE, B-4000 Liège, Belgium

Abstract

The RIVERSTRAHLER model, an idealized biogeochemical model of the river system, has been coupled to MIRO-CO_2, a complex biogeochemical model describing diatom and *Phaeocystis* blooms and carbon and nutrient cycles in the marine domain, to assess the dual role of changing nutrient loads and increasing atmospheric CO_2 as drivers of air–sea CO_2 exchanges in the Southern North Sea with a focus on the Belgian coastal zone (BCZ). The whole area, submitted to the influence of two main rivers (Seine and Scheldt), is characterized by variable diatom and *Phaeocystis* colonies blooms which impact on the trophic status and air–sea CO_2 fluxes of the coastal ecosystem. For this application, the MIRO-CO_2 model is implemented in a 0D multibox frame covering the eutrophied Eastern English Channel and Southern North Sea and receiving loads from the rivers Seine and Scheldt. Model simulations are performed for the period between 1951 and 1998 using real forcing fields for sea surface temperature, wind speed and atmospheric CO_2 and RIVERSTRAHLER simulations for river carbon and nutrient loads. Model results suggest that the BCZ shifted from a source of CO_2 before 1970 (low eutrophication) towards a sink during the 1970–1990 period when anthropogenic DIN and P loads increased, stimulating C fixation by autotrophs. In agreement, a shift from net annual heterotrophy towards autotrophy in BCZ is simulated from 1980. The period after 1990 is characterized by a progressive decrease of P loads concomitant with a decrease of primary production and of the CO_2 sink in the BCZ. At the end of the simulation period, the BCZ ecosystem is again net heterotroph and acts as a source of CO_2 to the atmosphere. R-MIRO-CO_2 scenarios testing the relative impact of temperature, wind speed, atmospheric CO_2 and river loads variability on the simulated air–sea CO_2 fluxes suggest that the trend in air–sea CO_2 fluxes simulated between 1951 and 1998 in the BCZ was mainly controlled by the magnitude and the ratio of inorganic nutrient river loads. Quantitative nutrient changes control the level of primary production while qualitative changes modulate the relative contribution of diatoms and *Phaeocystis* to this flux and hence the sequestration of atmospheric CO_2.

Keywords: air-sea CO2 fluxes, Carbon dioxide, coastal zone, eutrophication, North Sea

Received 14 March 2008; revised version received 22 August 2008 and accepted 22 September 2008

Introduction

Despite its relatively modest surface area, the coastal zone plays a considerable role in the carbon and nutrient global biogeochemical cycles. At the interface between land, atmosphere and the open ocean, the coastal zone receives massive inputs of terrestrial organic matter and nutrients that stimulate intense biological processes (Smith & Hollibaugh, 1993; Gattuso *et al*., 1998; Wollast, 1998) and exchanges nutrients and inorganic and organic carbon with the open ocean across marginal boundaries (e.g. Wollast, 1998; Thomas *et al*., 2004) and the sediment (Wollast, 1998; Chen *et al*., 2003; Middelburg & Soetaert, 2004; Middelburg *et al*., 2005). The coastal zone is also the area of greatest

Correspondence: N. Gypens, tel. +32 26505924, fax +32 26505993, e-mail: ngypens@ulb.ac.be

human impact on the marine environment as approximately 40% of the human population is currently living within 100 km of the coastline (Cohen *et al*., 1997).

During the last century, increase of human activities on land (combustion of fossil fuels, prolonged and intensive use of inorganic fertilizer in agriculture, changes in land use practices, deforestation and discharge of industrial and municipal waste waters) has caused substantial increase in atmospheric CO_2 concentration and affected river nutrient and carbon fluxes (e.g. Mackenzie *et al*., 2002). Anthropogenic disturbance has lead to an increased delivery of inorganic nutrients and organic carbon into estuaries and coastal waters (van Beusekom & de Jonge, 2002; Smith *et al*., 2003) and contributed to their eutrophication (Cloern, 2001). This phenomenon has led to severe degradation of water quality and alteration of the marine food web and community structure (e.g. Officer & Ryther, 1980; Billen *et al*., 1991; Cloern, 2001). The excess of nutrient may locally enhance primary production and carbon sequestration but the modification of organic carbon loads can also considerably influence the carbon metabolism changing the autotrophic vs. heterotrophic conditions in estuaries and coastal waters (Heip *et al*., 1995; Kemp *et al*., 1997) and hence their ability to pump atmospheric CO_2 (Andersson & Mackenzie, 2004; Mackenzie *et al*., 2004).

The environmental consequences of nutrient enrichment of coastal ecosystems (e.g. increased phytoplankton production, increased turbidity with subsequent loss of submerged aquatic vegetation, oxygen deficiency, decreased in biodiversity, etc.) are becoming increasingly well documented (e.g. Nixon, 1995; Vitousek *et al*., 1997; Cloern, 2001) but the role of the coastal zone as source or sink for atmospheric CO_2 is the subject of a long-lived controversy that mainly originates from the lack of sufficient field measurements, their probable inadequate spatial and/or seasonal coverage and the diversity and complexity of this marine realm from the point of view of carbon cycling (Borges, 2005; Borges *et al*., 2005, 2006). The estimation of the CO_2 exchange across the air–sea interface in coastal areas differs between authors and their potential contribution to the ocean uptake of CO_2 remains uncertain (Borges, 2005; Cai *et al*., 2006; Chen & Borges, 2008). Moreover, the modification of the capacity of coastal waters to absorb atmospheric CO_2 due to increased human pressure also remains poorly known. Some model studies exploring the impact of increased nutrient and carbon loads on the heterotrophic or autotrophic status (Ver *et al*., 1999; Rabouille *et al*., 2001) and the direction of the air–sea CO_2 exchanges in the global coastal area over the past 300 years (Andersson & Mackenzie, 2004; Mackenzie *et al*., 2004) conclude that the ecosystem trophic status and air–sea CO_2 exchanges have changed since the industrial revolution. In spite of some uncertainties, these studies show that worldwide coastal waters have probably acted as a net CO_2 source to the atmosphere for much of the past 300 years, but have recently switched, or will switch soon, to a net sink of CO_2, because of rising atmospheric CO_2 and eutrophication. These studies neither consider the diversity of the coastal zone ecosystem nor the variations of local anthropogenic pressure. Consequently, although these studies give a general overview of the coastal zone response to the worldwide anthropogenic modification over the last centuries, they do not consider the response of a specific coastal ecosystem, in particular if nutrient reduction measures are taken to reduce eutrophication. As a first step in this direction, da Cunha *et al*. (2007) recently explored the potential impact of changes in river nutrient loads on global ocean biogeochemistry using a more detailed global model compared with the previous simple box-models (Ver *et al*., 1999; Rabouille *et al*., 2001). However, this study only considers N and Si (and Fe) as potential limiting nutrients, preventing the transposition of their results to eutrophied coastal areas where P can be limiting due to high N : P ratios (Howarth & Marino, 2006; Gypens *et al*., 2007).

The Belgian coastal zone (BCZ) located in the Southern Bight of the North Sea receives freshwater and nutrient loads from anthropized rivers (mainly the Seine and the Scheldt) that mix with inflowing English Channel waters (Fig. 1). Over the last five decades, nutrient river loads have been modified in quantity and quality (large excess of nitrate and phosphate over silicate; Billen *et al*., 2001, 2005; Soetaert *et al*., 2006) due to increased human activity and the implementation of nutrient reduction (especially P) policies in the mid-1980s. These changing nutrient inputs have shaped the structure and the functioning of the BCZ ecosystem, characterized today by the dominance of undesirable *Phaeocystis* blooms (Lancelot, 1995). Model reconstruction of eutrophication suggests that *Phaeocystis* colonies were already blooming in BCZ in the early 1950s but were sharing almost equally with diatoms, the bulk of annual primary production (Lancelot *et al*., 2007). Over the 1960–1992 period, the increased loads of both N and P were largely beneficial to both *Phaeocystis* colonies and summer diatoms, however, with a little advantage to the latter. Since 1989, the decrease in P loads subsequent to the removal of PO_4 in washing powders and the maintenance of elevated NO_3 loads led to a larger decrease of diatom than *Phaeocystis* blooms, leading to their present-day dominance (Lancelot *et al*., 2007). However, the extent to which these historical changes in the phytoplankton community structure were affecting the BCZ ability to absorb atmospheric CO_2 is not

known. Measurements of the partial pressure of surface CO_2 (pCO_2) obtained in the BCZ during the late 1990s and early 2000s (the period of P reduction) evidenced that pCO_2 in the area was seasonally driven by both fresh water inputs from the Scheldt and biological activities (Borges & Frankignoulle, 1999, 2002, 2003; Schiettecatte *et al*., 2006). Annual budgets for the period report the coastal area as a source of CO_2 to the atmosphere and suggest that the interannual variation of this source is related to Scheldt discharge fluctuations (Borges & Frankignoulle, 1999). This suggests that the human-driven changing nutrient loads over the last 50 years might well have affected the capacity of the coastal area to absorb atmospheric CO_2 but the pCO_2 time series available for the area is too short for appraising this effect.

In this paper, we use the MIRO-CO_2 biogeochemical model of Gypens *et al*. (2004) describing the seasonal evolution of pCO_2 in the BCZ surface waters to assess and understand the evolution over the past 50 years of air–sea CO_2 flux in the BCZ in response to increased atmospheric pCO_2 and changes in river carbon and nutrient loads and in coastal ecosystem structure. For this application, we use recorded sea surface temperature, wind speed, atmospheric CO_2 and RIVERSTRAHLER simulations of carbon and nutrient rivers loads from the Seine and the Scheldt (Billen *et al*., 2001, 2005) to simulate the seasonal and interannual evolution of air–sea CO_2 fluxes in the BCZ during the 1951–1998 period. RIVERSTRAHLER–MIRO-CO_2 results are then analysed to estimate the relative contribution of these drivers (increased atmospheric CO_2 and changing nutrient loads) to the interannual variability of the simulated air–sea CO_2 fluxes.

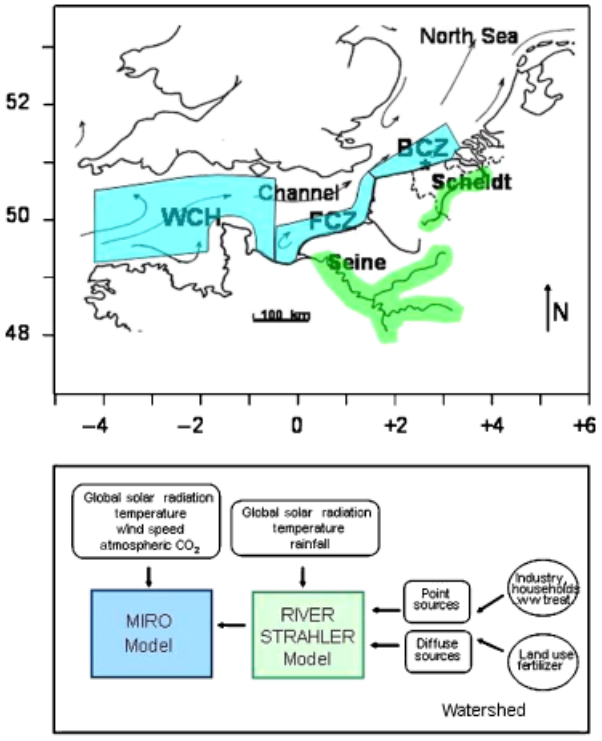

Fig. 1 Map of the study area with the MIRO multibox frame delimitation (top panel) and the RIVESTRAHLER–MIRO-CO_2 coupling (bottom panel). WCH, Western Channel; FCZ, French coastal zone; BCZ, Belgian coastal zone.

Material and methods

Mathematical models

The mathematical tool consists in the coupling of the coastal MIRO-CO_2 model (Gypens *et al*., 2004) and the RIVERSTRAHLER river model (Billen *et al*., 1994; Garnier *et al*., 1995): the RIVERSTRAHLER–MIRO-CO_2 tool (R-MIRO-CO_2). This coupling is possible because of the structural similarity of the two idealized models (Lancelot *et al*., 2007). R-MIRO-CO_2 (Fig. 1) allows the description of biogeochemical transformations of C, N, P and Si along the river–coastal continuum as a function of changing human activity in the watershed.

The RIVERSTRAHLER model. RIVERSTRAHLER (Billen *et al*., 1994; Garnier *et al*., 1995) is a generic model of the biogeochemical functioning of the whole river system resulting from the coupling of a hydrological module (HYDROSTRAHLER) and a biogeochemical module (RIVE). Structure and parameterization of RIVE processes are detailed in Garnier *et al*. (1999, 2002). The implementation of RIVERSTRAHLER and a description of the meteorological forcing and nutrient point and diffuse sources at the scale of the Seine and Scheldt river systems over the past 50 years are reported in Billen *et al*. (2001, 2005). For both basins, the model-forcing functions to the model were collated for the period 1951–1998: year-to-year variation of rainfall by 10-day steps; land use modifications by 10-year steps; changes in urban and industrial annual wastewater discharges by 5-year steps. The simulated nutrient loads were validated by comparison with annual nutrient loads recorded at the river mouths (Lancelot *et al*., 2007).

The MIRO-CO_2 model. The MIRO-CO_2 biogeochemical model (Gypens *et al*., 2004) results from the coupling of the biogeochemical MIRO model (Lancelot *et al*., 2005) with the physicochemical module of Hannon *et al*. (2001), describing the seawater carbonate system and air–sea CO_2 exchange. The mechanistic biogeochemical MIRO model, describing C, N, P and Si cycles in

Phaeocystis-dominated ecosystems, assembles four modules, describing the dynamics of phytoplankton (diatoms, nanoflagellates and *Phaeocystis*), zooplankton (copepods and microzooplankton), dissolved and particulate organic matter (each with two classes of biodegradability) degradation and inorganic nutrients [NO_3, NH_4, PO_4 and $Si(OH)_4$] regeneration by bacteria in the water column and the sediment. The MIRO equations and parameters are fully documented in Lancelot *et al*. (2005) and www.int-res.com/journals/suppl/appendix_lancelot.pdf. A first coupling between MIRO and RIVERSTRAHLER demonstrated the ability of the model to reproduce the observed evolution of nutrients and *Phaeocystis* and diatom blooms during the 1988–1998 period (Lancelot *et al*., 2007).

The speciation of the carbonate system (in particular pCO_2) is calculated from dissolved inorganic carbon (DIC) and total alkalinity (TA), using the carbonic acid dissociation constants recommended by Mehrbach *et al*. (1973), the boric acid dissociation constants given by Dickson (1990) and the CO_2 solubility coefficient suggested by Weiss (1974). Air–sea CO_2 fluxes are calculated from the pCO_2 gradient across the air–sea interface ($\Delta pCO_2 = pCO_2 - pCO_{2atm}$, where pCO_{2atm} refers to values in the atmosphere) and the gas transfer velocity parameterization as a function of wind speed of Nightingale *et al*. (2000).

Model implementation

For this application, the R-MIRO-CO_2 model is implemented in a multibox frame delineated on the basis of the hydrological regime and river inputs. In order to take into account the cumulated nutrient enrichment of Atlantic waters by the Seine and Scheldt rivers, two successive boxes, assumed to be homogeneous, have been chosen from the Seine Bight (French coastal zone, FCZ) to the BCZ (Fig. 1). Each box has its own morphological characteristics (Lancelot *et al*., 2005) and is treated as an open system, receiving waters from the upward adjacent box and the river (Seine or Scheldt) discharge and exporting water to the downward box. Model simulations were performed over the 1951–1998 period after a 3-year spin-up run. The boundary conditions were provided by the MIRO-CO_2 simulations performed for the conditions existing in the Western Channel (WCH; Fig. 1), which is considered to be a quasioceanic closed system. The time evolution of the state variables was calculated by solving the different equations expressing mass conservation according to the Euler procedure. A time step of 15 min was adopted for the computation of the numerical integration. Model runs were performed using recorded daily wind speed, sea surface temperature, monthly atmospheric pCO_2 and 10-day river (Seine and Scheldt) loads calculated by the RIVERSTRAHLER model. Because of the lack of data, a climatology corresponding to the 1989–1999 period (Lancelot *et al*., 2005) was used as global solar radiation. Land-based fluxes of DIC and TA were estimated based on a compilation of DIC and TA data in the Seine and the Scheldt rivers (Frankignoulle *et al*., 1996, 1998; Frankignoulle & Borges, 2001; A. V. Borges unpublished data; G. Abril, personal communication) and river discharges, making use of the 'apparent zero end-member' method (Kaul & Froelich, 1984). The 'apparent zero end-member' concentration of DIC and TA was computed as the y-intercept of the linear regression of these quantities as a function of salinity for values between 15 and 30. Such an approach allows computing realistic river fluxes to the coastal zone, by removing the effect of nonconservative behaviour of chemicals in upper estuaries (e.g. TA in the Scheldt estuary; Frankignoulle *et al*., 1996) that leads to erroneous estimates if the real concentration at zero salinity is used. Because of the scarcity of TA and DIC data in the Seine river, constant concentrations of these quantities were used to compute the river fluxes. For the Scheldt river, linear regressions of DIC or of TA as a function of the logarithm of freshwater discharge (Q) were used to determine the concentration of DIC or TA for a given Q value:

$$\begin{aligned} &\mathrm{DIC} = 5.377 - 0.5992 \log(Q) \\ &(r^2 = 0.67,\ P < 0.0001,\ n = 19) \\ &\mathrm{TA} = 4.907 - 0.4584 \log(Q) \\ &(r^2 = 0.56,\ P = 0.0003,\ n = 19) \end{aligned},$$

where DIC and TA are in mmol kg^{-1} and Q in $m^3\,s^{-1}$ is the average over the 2 months before sampling based on 19 cruises from 1993 to 2000.

The negative relationships between DIC or TA and Q are due to the dilution of these quantities during flood events, typical of most rivers (Ludwig *et al*., 1996; Cai *et al*., 2008).

Wind speed was extracted from the National Centers for Environmental Prediction (NCEP) Reanalysis Daily Averages Surface Flux (http://www.cdc.noaa.gov/) for one station in the North Sea (3.75°E, 52.38°N). Atmospheric pCO_2 at Mace Head (53.55°N, 9.00°W, Southern Ireland) was provided by the National Oceanic and Atmospheric Administration/Climate Monitoring and Diagnostics Laboratory/Carbon Cycle Greenhouse Gases Group (NOAA/CMDL/CCGG) air-sampling network (available at http://www.cmdl.noaa.gov/) for the 1979–1998 period. Years before 1979 were reconstructed by assuming a similar annual increase rate as measured at Mauna Loa (http://www.esrl.noaa.gov/). Values of pCO_{2atm} in dry air were

converted into pCO_{2atm} in wet air according to Dickson & Goyet (1994). Annual mean seawater temperature was derived from the ICES report on Ocean Climate 2005 (no. 280) and daily cycle was reconstructed based on the mean daily seawater temperature cycle measured in the area during the 1989–1999 period (Lancelot *et al.*, 2005).

Sensitivity scenarios

The relative impact of the different model forcing on the ecosystem trophic status and air–sea CO_2 flux simulated between 1951 and 1998 in the BCZ was assessed by testing separately the 1951 value for each forcing. In the manuscript, nine scenarios will be distinguished on the basis of the tested 1951 forcing (Table 1). In each of these scenarios, the 1951 value was used for the tested forcing, but real values were used for the other forcings.

Statistical analysis

The results of the sensitivity scenarios have been statistically valuated using the Taylor's (2001) diagram. This diagram summarizes visually the degree of correspondence between two fields, in our case between reference and model scenarios, allowing to rank the effect of the different forcings on the real historical evolution of the air–sea CO_2 fluxes in BCZ. Similarity between two simulations (f, the sensitivity scenario and r, the reference) is estimated based on three complementary, but not completely independent, statistics:

Table 1 Nine test model scenarios

Tested 1951 forcing	Scenario name	Scenario symbol
Seawater temperature	T-scenario	A
Wind speed	WS-scenario	B
Atmospheric pCO_2	CO_2-scenario	C
Seine and Scheldt C and nutrient loads	R-scenario	D
Seine and Scheldt DIN loads	N-scenario	E
Seine and Scheldt PO_4 loads	P-scenario	F
Seine and Scheldt organic C loads	C-scenario	G
Scheldt C and nutrient loads	Scheldt-scenario	H
Seine C and nutrient loads	Seine-scenario	I

In each of these scenarios, the 1951 value was used for the tested forcing, but real values were used for the other forcings.

- the correlation coefficient (R) is used to quantify pattern similarity between the two simulations:

$$R = \frac{(1/N)\sum_{n=1}^{N}(f_n - \bar{f})(r_n - \bar{r})}{\sigma_f \sigma_r},$$

where $\bar{f}$ and $\bar{r}$ are the mean values and σ_f and σ_r are the standard deviation of f and r, respectively, and N is the number of values to be considered.

- the variance of the two simulations (σ_f and σ_r) allows to determine whether two results have the same amplitude of variation.
- the centred pattern root mean square (RMS) difference (E') quantifies the difference between the two simulations:

$$E' = \left\{\frac{1}{N}\sum_{n=1}^{N}[(f_n - \bar{f})^2 - (r_n - \bar{r})^2]^{1/2}\right\},$$

The above statistics (R, E', σ_f, σ_r) are related as:

$$E'^2 = \sigma_f^2 + \sigma_r^2 - 2\sigma_f \sigma_r R.$$

and can then be geometrically represented in a single diagram based on the law of Cosines, the Taylor's (2001) diagram (Fig. 2).

The correspondence between any scenario and the reference simulation can be seen by analysing the position of one single point on the diagram (Fig. 2). The azimuthal position of the model scenario indicates the correlation (the smaller the angle, the better is the correspondence), its distance from the origin indicates its standard deviation and the distance between the *Scenario* and the *Reference* symbols is related to the centred pattern RMS difference (E'). Standard deviation and E' are nondimensionalized by the standard deviation of the reference simulation. In the limit of a perfect agreement between the two simulations, E' would approach 0, and σ and R the unit and the tested forcing has no impact on the long-term trend of annual air–sea CO_2 fluxes.

Results

R-MIRO-CO_2 simulations for the 1951–1998 period

Seine and Scheldt loads. Figure 3 shows the 1951–1998 evolution of annual fresh water discharge and annual total nitrogen (Ntot), phosphorus (Ptot), dissolved silicate (DSi) and organic carbon loads simulated by the RIVERSTRAHLER model applied to the Seine and the Scheldt watersheds. The annual carbon and nutrient fluxes delivered by the Scheldt and the Seine show similar historical trends but the magnitude of the simulated nutrient loads of the Seine is in averaged

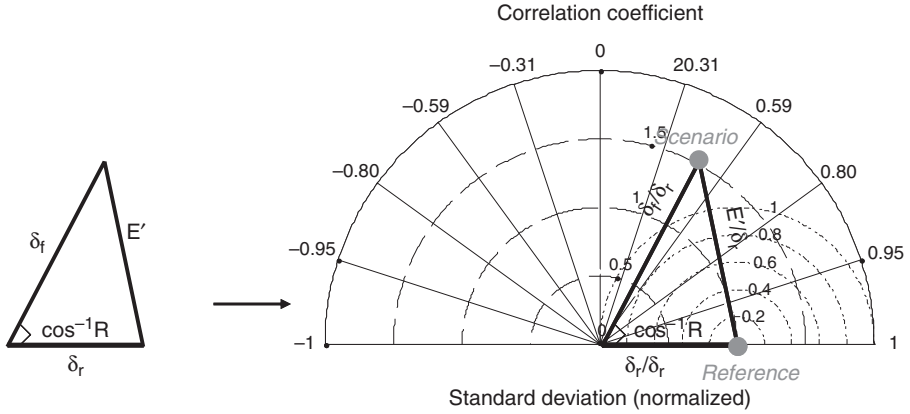

Fig. 2 Taylor diagram. *Left*: geometric relationship between the correlation coefficient R, the standard deviation δ_f and δ_r of the model scenario and the reference simulation and the centred pattern root mean square (RMS) error E'. *Right*: normalized diagram. The radial distance from the origin is proportional to the normalized standard deviation (δ_f/δ_r). The normalized RMS difference (E'/δ_r) between the *Scenario* and the *Reference* simulation is proportional to their distance apart and their correlation is given by the azimuthal position of the *Scenario* simulation.

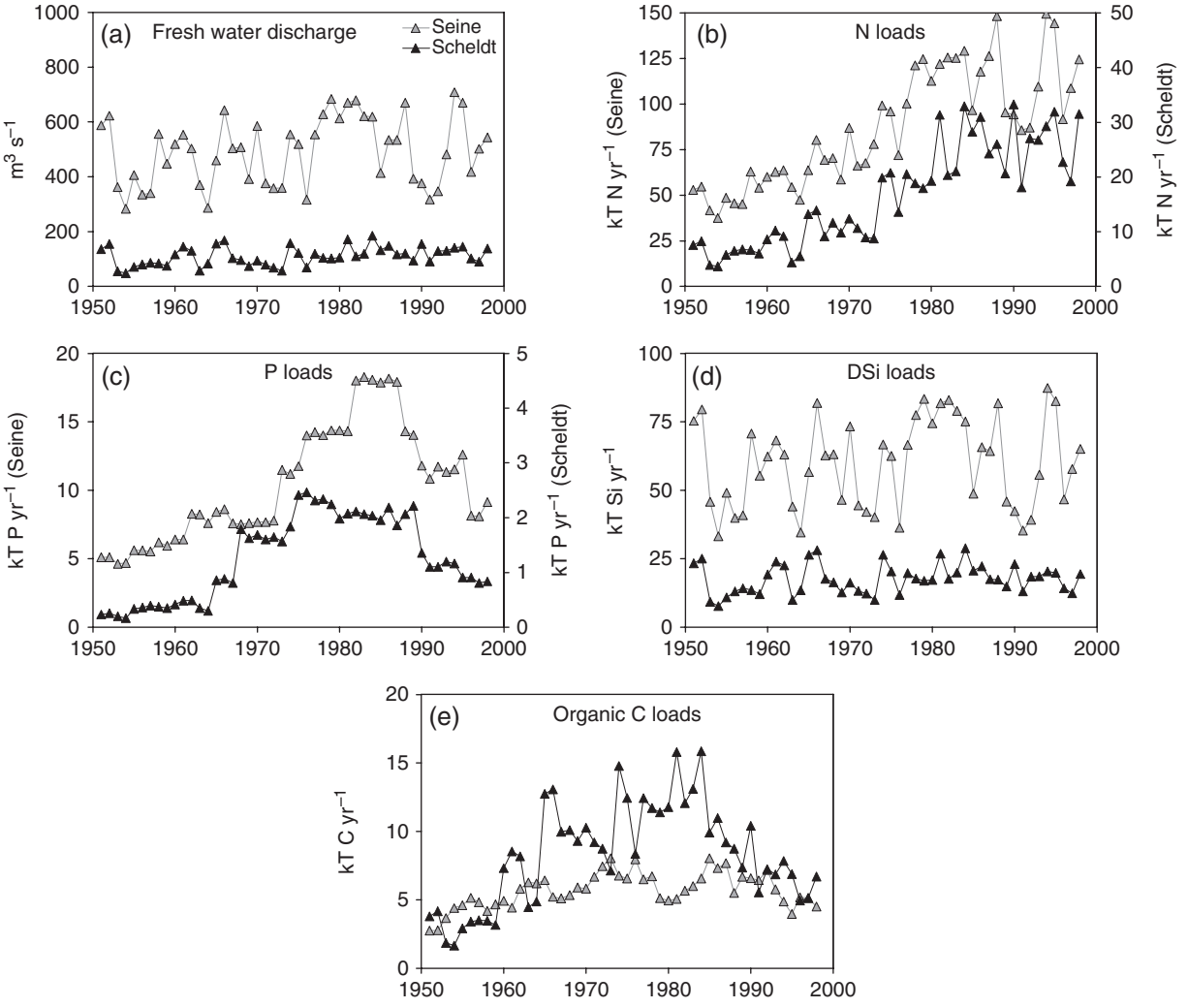

Fig. 3 Evolution from 1951 to 1998 of annual fresh water discharge (a) and Ntot (b), Ptot (c), DSi (d) and organic carbon (e) annual loads from the Seine (grey) and the Scheldt (black).

for the period 5 (Ntot; Fig. 3b), 10 (Ptot, Fig. 3c) and 3 (Dsi; Fig. 3d) times higher than for the Scheldt. This mainly results from a higher water discharge from the Seine than the Scheldt (Fig. 3a) while nutrient concentrations are similar in both rivers (not shown). Interestingly, specific nutrient loads, that is, normalized with respect to the watershed surface area, show similar values and historical trends for the two watersheds (Billen *et al.*, 2001, 2005). On the contrary, organic carbon inputs simulated for the Scheldt are up to three times higher than the Seine loads during the 1980s (Fig. 3e). Although some part of the interannual variability of nutrient and organic carbon loads can be attributed to the variability of the river water discharge (Fig 3a), the long-term trend simulated during the past 48 years is responding to modification of human activities in the watershed.

From 1951 to the mid-1960s, Ntot (Fig. 3b), Ptot (Fig. 3c) and DSi (Fig. 3d) loads show little variation for the Seine and the Scheldt rivers. After 1965 and as a result of the combined effect of increased leaching of agricultural soils and emissions from domestic and industrial activities (Billen *et al.*, 2001, 2005), the annual Ntot fluxes delivered by the Seine (Fig. 3b) increase from some $50\,kT\,N\,yr^{-1}$ in the 1950–1960s up to values $>100\,kT\,N\,yr^{-1}$ during the 1980s and 1990s. A similar increase is simulated for the Scheldt with Ntot loads $<10\,kT\,N\,yr^{-1}$ before 1973 and $\sim 30\,kT\,N\,yr^{-1}$ from 1980 onwards (Fig. 3b). The annual Ptot simulated for the Seine and the Scheldt suggests four successive phases (Fig. 3c): (i) the 1951–1965 period of low input; (ii) the increased delivery period (i.e. from $5\,kT\,P\,yr^{-1}$ before 1965 up to $17\,kT\,P\,yr^{-1}$ in 1980 for the Seine and from $0.5\,kT\,P\,yr^{-1}$ before 1965 up to $2.6\,kT\,P\,yr^{-1}$ from mid-1970s for the Scheldt); (iii) the period of sustained elevated inorganic nutrient loads; and (iv) the progressive decrease until 1998 when the values from the 1960s are again simulated. This decrease results from the removal of PO_4 in washing powders, as well as from the improved treatment of urban effluents (Billen *et al.*, 2001, 2005). DSi loads show important interannual variability (Fig. 3d) mainly driven by freshwater discharge (Fig. 3a), while DSi concentration, little affected by human activity, shows little variation in each river (not shown). Organic carbon loads, as Ntot and Ptot loads, show, after 1960, a marked increase in response to human development on the watershed before decreasing from the mid-1980s onwards in response to waste water treatment (Fig. 3e).

Carbon fluxes in BCZ. Over the simulated period, atmospheric pCO_2 increased from a mean annual value of ~ 310 ppm in 1951 to values >370 ppm in 1998 (Fig. 4). Meanwhile, the R-MIRO-CO_2 simulated

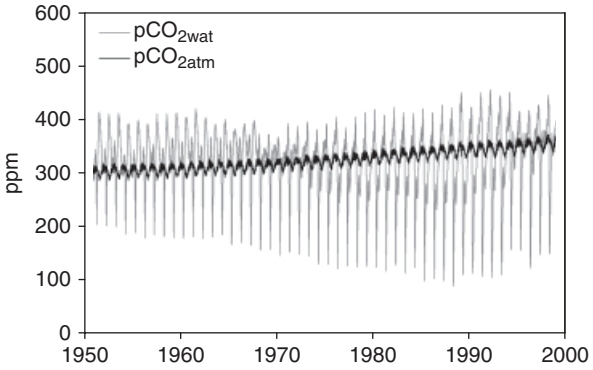

Fig. 4 Evolution from 1951 to 1998 of pCO_2 simulated by R-MIRO-CO_2 in the Belgian coastal zone (BCZ) and pCO_{2atm} measured at Mace Head.

water pCO_2 (pCO_{2wat}) shows large seasonal and interannual fluctuations (Fig. 4). As a general trend, undersaturation is simulated in spring while oversaturation is maximal in winter. Over the long-term, the maximal winter pCO_{2wat} remains relatively constant (~ 400 ppm), while spring undersaturation shows over years two opposite trends: an increase of pCO_{2wat} undersaturation from 200 ppm during the 1950s and 1960s down to 100 ppm during the late 1980s followed after 1989 by a decreasing trend of the undersaturation (~ 50 ppm over 8 years, Fig. 4).

Under or oversaturation of surface water pCO_2 results from an imbalance between photosynthetically fixed CO_2 and respired organic carbon due to heterotrophic activity. When calculated over the year, this difference, the net ecosystem production (NEP), gives an indication on the autotrophic or heterotrophic status of the water body. Figure 5a shows the 1951–1998 evolution of the NEP calculated from R-MIRO-CO_2 simulations of annual photosynthesis and respiration rates.

Annual NEP in the BCZ computed with R-MIRO-CO_2 shows important interannual variability between 1951 and 1998, with values ranging between -1.24 and $+0.44\,mol\,C\,m^{-2}\,yr^{-1}$ in 1966 and 1989, respectively (Fig. 5a). Between 1951 and 1967, the BCZ ecosystem is the net heterotrophic with an annual NEP ranging between -0.68 and $-1.24\,mol\,C\,m^{-2}\,yr^{-1}$. After 1967, the ecosystem is still heterotroph but the magnitude is less significant with annual NEP values of $-0.2\,mol\,C\,m^{-2}\,yr^{-1}$ in 1982. Between 1983 and 1993, the BCZ ecosystem alternates between heterotrophy and autotrophy with the highest net autotrophy simulated in 1989 and 1992 ($NEP > +0.3\,mol\,C\,m^{-2}\,yr^{-1}$). After 1993 and up to the end of the simulated period, the direction of NEP is reverted and the magnitude of the simulated annual heterotrophy is similar to that simulated before 1967 except in 1996 when net heterotrophy decreases.

At a first glance, the simulated interannual fluctuations of air–sea CO_2 fluxes (Fig. 5b) mirror those obtained for the NEP over the 1951–1998 period (Fig. 5b). Between 1951 and end 1960, the BCZ annually acts as a source for atmospheric CO_2, ranging between 0.03 and 0.50 mol C m^{-2} yr^{-1}. However, after 1966 the magnitude of the CO_2 source shows an abrupt decrease of 0.125 mol C m^{-2} yr^{-1}, reaches 0 in 1970 and maintains the null balance up to 1974 (Fig. 5b). From 1975 to 1993, the BCZ is absorbing atmospheric CO_2 with a maximal value of −0.4 mol C m^{-2} yr^{-1} in 1985, after that the magnitude of the sink gradually decreases. Between 1994 and 1998, a net source of CO_2 is again simulated ranging between 0.06 and 0.18 mol m^{-2} yr^{-1}, except in 1996.

Mechanisms driving the interannual and long-term variability of air–sea CO_2 fluxes in BCZ between 1951 and 1998

Sea surface temperature, wind speed, atmospheric CO_2 and carbon and nutrient loads directly or/and indirectly constrain air–sea CO_2 fluxes. Wind speed acts on the gas transfer velocity affecting the intensity of the air–sea CO_2 flux. The direction of air–sea CO_2 flux depends on the air–sea gradient of pCO_2 that is a function of atmospheric CO_2 and seawater pCO_2. Seawater pCO_2 will depend of sea surface temperature (solubility coefficient) and of biological activity function of carbon and inorganic nutrient inputs. The contribution of each of these forcings to the simulated annual air–sea CO_2 flux is investigated based on the comparison between real R-MIRO-CO_2 simulations obtained for the1951–1998 period (= reference simulation) and those obtained by running R-MIRO-CO_2 with the 1951 values of either sea surface temperature, wind speed, atmospheric CO_2 or carbon and/or nutrient loads for each year of the considered period (= 9 scenarios defined in 'Sensitivity scenarios').

Interannual variability. Sea surface temperature (Fig. 6b) and wind speed (Fig. 6d) recorded over the 1951–1998 period fluctuated between −1.2 and 1.3 °C, and −0.4 and 0.6 m s^{-1} of their 1951 values, while pCO_{2atm} regularly increased by 55 ppm (Fig. 6f). The comparison of annual air–sea CO_2 fluxes simulated using real and 1951 values of sea surface temperature (T-scenario; Fig. 6a), wind speed (WS-scenario; Fig. 6c) and atmospheric pCO_2 (CO_2-scenario; Fig. 6e) suggests that the interannual variability of these forcings has little impact on the magnitude and the direction of the simulated air–sea CO_2 flux and no influence on the simulated long-term trend. Similarly, sea surface temperature variability has no major influence on the long-term trend of annual NEP that shows similar patterns when using real and 1951 forcings (not shown). Figure 6b, d and f compare the delta annual air–sea CO_2 flux (i.e. the difference between model results obtained using real and 1951 forcing values) with delta annual temperature, wind speed or atmospheric CO_2, respectively. Temperature variability contributes up to 0.2 mol C m^{-2} of the annual air–sea CO_2 (Fig. 6a) and the significant positive relationship ($r^2 = 0.85$, $P < 0.0001$) found between delta temperature and delta air–sea CO_2 fluxes is explained by the temperature control of the CO_2 solubility coefficient and hence the carbonate chemistry (Fig. 6b). The lack of relationship between the temperature-induced variability of the air–sea CO_2 flux and that of the NEP (not shown) suggests that on an annual basis, the effect of temperature variability on CO_2 chemistry is higher than on biological activity. Wind speed variability explains on average < 0.05 mol C m^{-2} yr^{-1} of the variability of the CO_2 flux excepted in 1990 and 1995

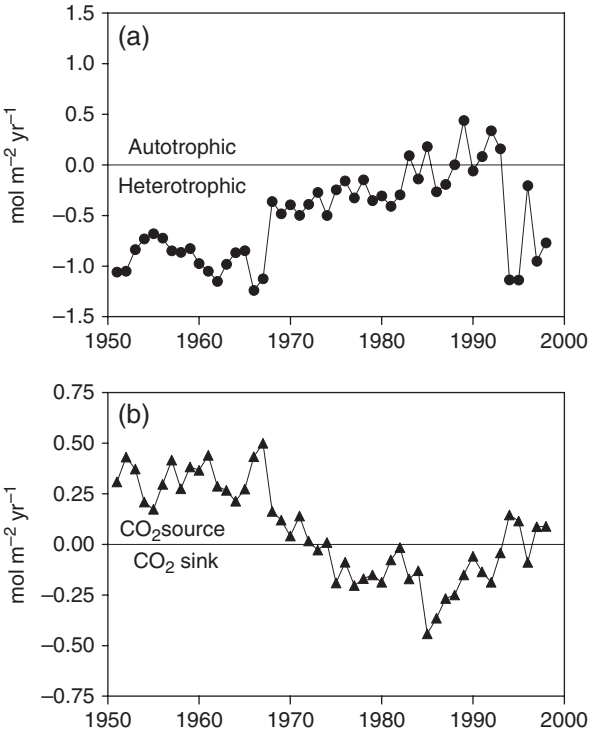

Fig. 5 Evolution from 1951 to 1998 of annual net ecosystem production (NEP) (a) and annual air–sea CO_2 fluxes (b) simulated by R-MIRO-CO_2 in the Belgian coastal zone (BCZ). Net ecosystem autotrophy corresponds to positive value of NEP and ecosystem heterotrophy to negative value. Air–sea CO_2 flux is positive when the flux is directed from the sea to the atmosphere (the area acts annually as a source for atmospheric CO_2) and a negative flux corresponds to an annual net sink for atmospheric CO_2 with a transfer of CO_2 from the atmosphere to the seawater.

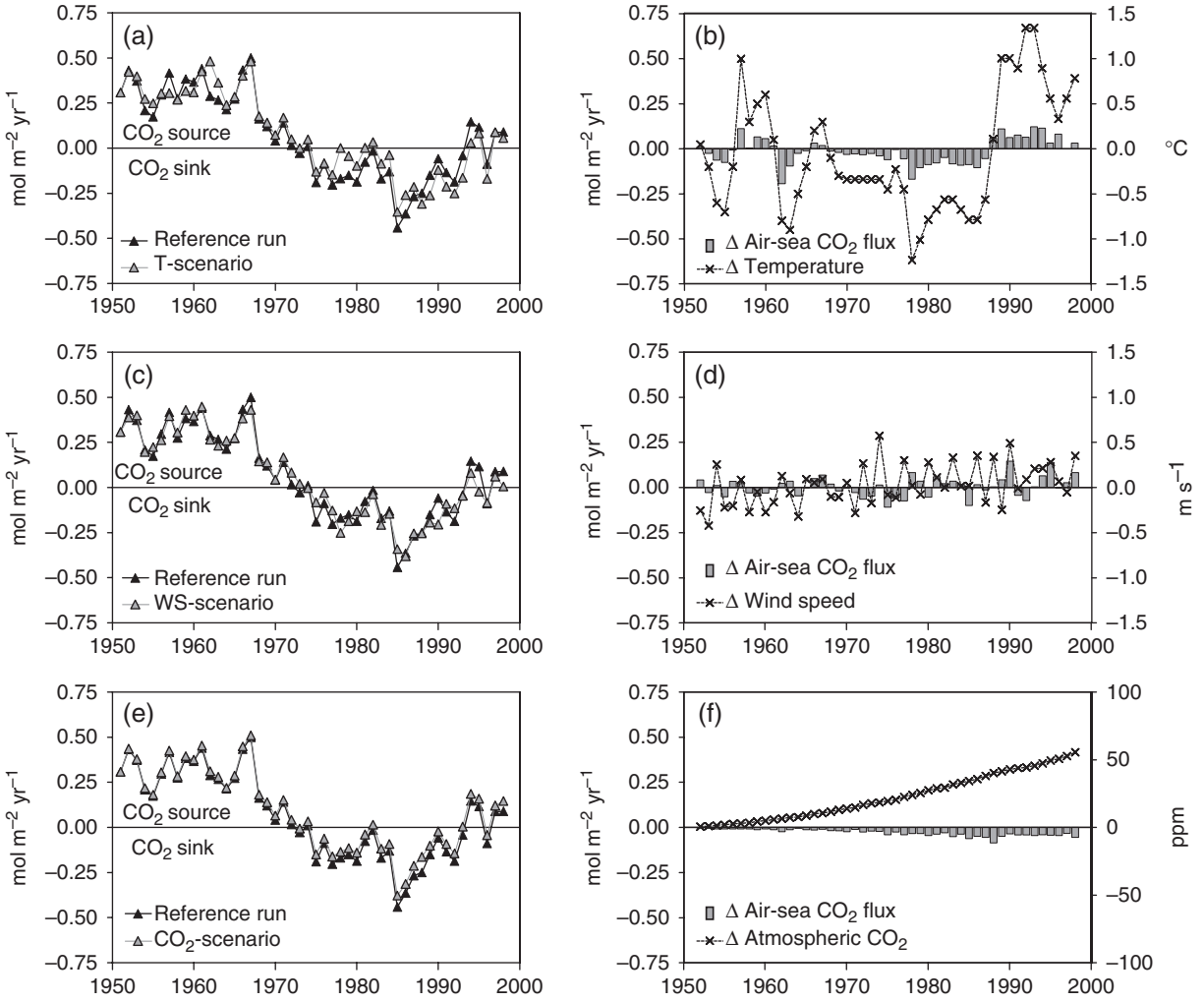

Fig. 6 Relative contribution of sea surface temperature, wind speed and atmospheric pCO_2 to air–sea CO_2 fluxes computed by R-MIRO-CO_2 in the Belgian coastal zone (BCZ) from 1951 to 1998. Comparison of air–sea CO_2 fluxes computed using real forcings (black) and 1951 (grey) value for sea surface temperature (a), wind speed (c) and atmospheric pCO_2 (e). Delta air–sea CO_2 flux (grey bar; computed as the difference between model results obtained using real and 1951 forcing values) compared with delta temperature (b), wind speed (d) and atmospheric CO_2 (f) (cross; computed as the difference between real forcing and 1951 value).

when wind speed variability is responsible for up to $0.15\,mol\,C\,m^{-2}\,yr^{-1}$ of the air–sea CO_2 flux (Fig. 6c). In shallow and permanently well-mixed ecosystem as the BCZ, wind speed will not affect vertical nutrient fluxes nor mixed layer depth (hence nor biological activity) and will only modulate the air–sea CO_2 intensity (gas transfer velocity) but not the direction of the air–sea CO_2 flux. Hence, no significant relationship was found between annual delta wind speed and delta air–sea CO_2 fluxes. As expected, the reported increase of pCO_{2atm} (Fig. 4) over the simulated period increases the BCZ uptake of atmospheric CO_2 (Fig. 6f) up to $0.09\,mol\,C\,m^{-2}\,yr^{-1}$ of the annual air–sea CO_2 flux in 1988. The delta pCO_{2atm} and the delta air–sea CO_2 flux are significantly correlated ($r^2 = 0.70$, $P < 0.0001$). If we except the years when the simulated reference air–water CO_2 fluxes are nearly zero (1972, 1974, 1982, 1990 and 1993; Fig. 5b) and when variability of one forcing can largely modify the flux in term of percent, then temperature, wind speed and atmospheric CO_2 variability explain in average, respectively, 31%, 24% and 18% of the annual CO_2 fluxes but have no effect on the historical trend of air–sea CO_2 flux simulated between 1951 and 1998.

Most of the simulated 1951–1998 variability of NEP and air–sea CO_2 fluxes is explained by fluctuations in river loads (Fig. 7). In the R-scenario that maintains the 1951 values of the loads from the Seine and the Scheldt for the whole period, the BCZ is net heterotrophic on an annual basis (Fig. 7a) and a source for atmospheric CO_2

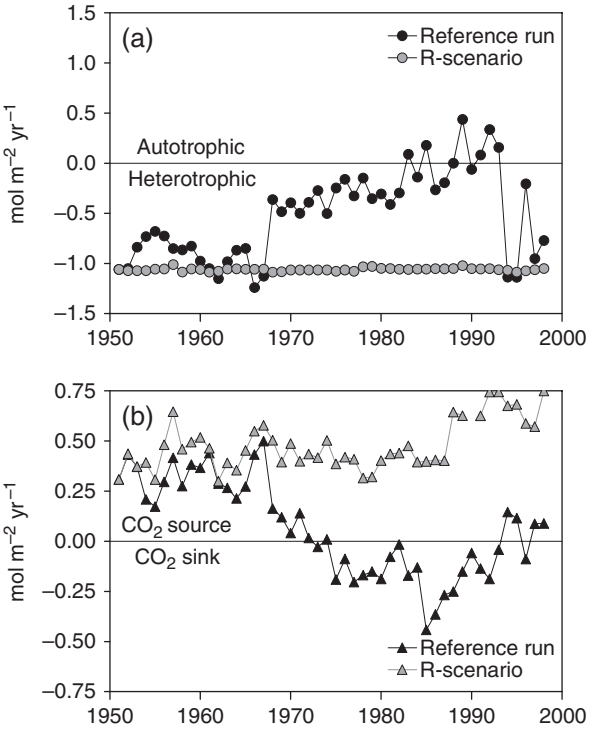

Fig. 7 Relative contribution of carbon and inorganic nutrient river loads to net ecosystem production (NEP) and air–sea CO_2 fluxes computed by R-MIRO-CO_2 in the Belgian coastal zone (BCZ) from 1951 to 1998. Comparison of (a) NEP and (b) air–sea CO_2 fluxes computed using real forcing (black symbols) and 1951 (grey symbols) value for Seine and Scheldt river loads.

(Fig. 7b), in spite of sea surface temperature, wind speed and atmospheric pCO_2 variability during the same period. In the R-scenario, the source of CO_2 increases between 1985 and 1998 due to the combined effect of wind speed and temperature changes that counteract the effect of increasing atmospheric CO_2 (that would decrease the CO_2 source). The increased delivery of river nutrient loads between 1951 and 1998 has a significant effect on the magnitude and the direction of the annual NEP and air–sea CO_2 flux (Fig. 7).

The relative influence of river nutrients and organic carbon loads on the simulated air–sea CO_2 fluxes in the BCZ was further investigated by running R-MIRO-CO_2 scenarios with either dissolved inorganic nitrogen (DIN; $NO_3 + NH_4$) (N-scenario), PO_4 (P-scenario) or organic carbon (C-scenario) loads of the Seine and the Scheldt corresponding to the year 1951. Results obtained were compared with the reference simulation (Fig. 8). As shown, the imposed constant DIN and PO_4 1951-loads predict positive annual air–sea CO_2 fluxes all along the simulated period (Fig. 8a and c). On the contrary, the use of 1951 carbon loads has little effect on air–sea CO_2 fluxes (Fig. 8e), suggesting that anthropogenic modification of organic carbon loads during the 1951–1998 period were of little significance for constraining air–sea CO_2 fluxes compared with nutrient load modifications. In agreement, the simulated delta air–sea CO_2 fluxes are low ($<0.1\,mol\,C\,m^{-2}\,yr^{-1}$; Fig. 8e) and are directly correlated to the delta organic carbon loads ($r^2 = 0.59$, $P < 0.0001$).

The sign and the magnitude of delta air–sea CO_2 fluxes are negatively related to the simulated delta nutrient loads of the Scheldt (Fig. 8b and d). DIN and PO_4 load increment over the simulated period is leading to a similar sink for atmospheric CO_2 (up to 0.8 and $0.7\,mol\,C\,m^{-2}\,yr^{-1}$, respectively, for DIN and PO_4; Fig. 8b and d) and the magnitude of this sink is positively correlated to the loads ($r^2 = 0.8$, $P < 0.0001$ for DIN and $r^2 = 0.68$, $P < 0.0001$ for PO_4). In both simulations, the magnitude of the atmospheric CO_2 sink is relatively low between 1952 and 1964, and gradually increases up to 1993 in response to the increase in DIN and PO_4 loads. After 1993, in spite of sustained elevated DIN loads but decreasing PO_4 loads, a decreasing trend of the atmospheric CO_2 sink is simulated in both scenarios (Fig. 8b and d).

Historical trends. The effect of the different forcings on the real historical evolution of the air–sea CO_2 fluxes in BCZ are quantitatively appraised using Taylor's (2001) diagram (Fig. 9). Statistics for the nine scenarios [correlation (R), their centred RMS difference (E') and the amplitude of their variations (standard deviation, σ)] were computed and positioned in the diagram. A letter was assigned to each scenario considered (Table 1). Each point on the diagram represents, for one particular scenario, the statistical analysis averaged over the entire period of simulation based on annual means. The more the scenario position is close to the reference, the less the considered forcing is constraining for determining the variability of the air–sea CO_2 flux between 1951 and 1998.

The very close position with respect to the reference of long-term simulations of annual air–sea CO_2 flux obtained by constraining R-MIRO-CO_2 with 1951 values of either atmospheric CO_2 (Fig. 9c) or organic carbon river loads (Fig. 9g) suggests that these forcings have seemingly little impact on the simulated 1951–1998 trend. Sea surface temperature (Fig. 9a) and wind speed (Fig. 9b) have little impact on the long-term trend of air–sea CO_2 fluxes, with $R > 0.95$, $E' < 0.35$ and standard deviation close to the unit. On the contrary, the position of scenarios using 1951 carbon and inorganic nutrient river loads forcing points, their significance for the control of the long-term trend of air–sea CO_2 fluxes, as R is close to 0, the standard deviation is close to 0.5 and E' is >1.1 (Fig. 9d). Interestingly, these statistical tests suggest a larger impact of nutrient and carbon loads delivered by the Seine (Fig. 9i) than by

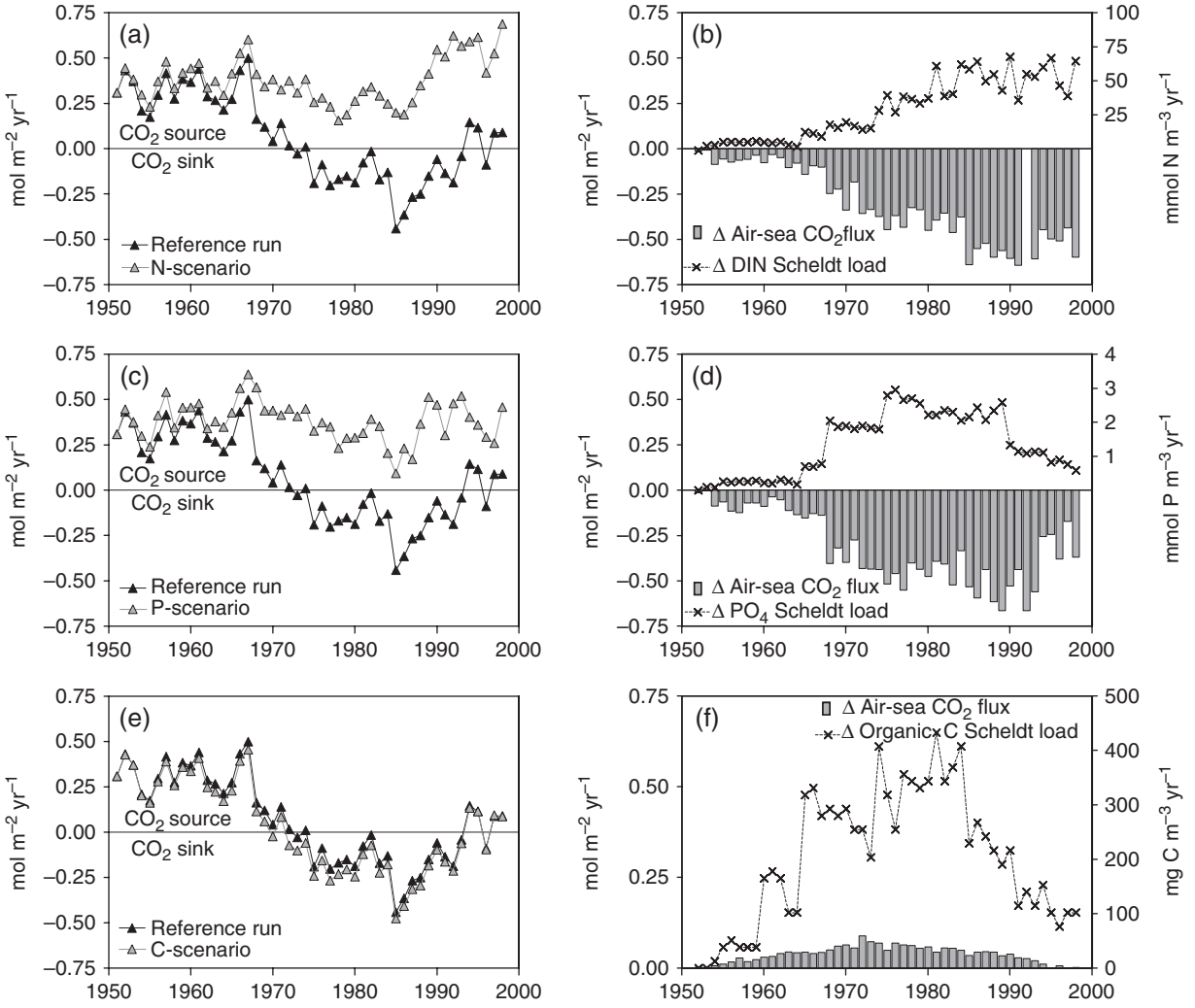

Fig. 8 Relative contribution of dissolved inorganic nitrogen (DIN), PO_4 and organic carbon Seine and Scheldt river loads to air–sea CO_2 fluxes computed by R-MIRO-CO_2 in the Belgian coastal zone (BCZ) from 1951 to 1998. Comparison of air–sea CO_2 fluxes computed using real forcing (black) and 1951 (grey) value for DIN (a), PO_4 (c) and organic carbon (e). Delta air–sea CO_2 flux (grey bar; computed as the difference between model results obtained using real and 1951 forcing values) compared with delta Scheldt loads of DIN (b), PO_4 (d) and organic carbon (f) (cross; computed as the difference between real forcing and 1951 value).

the Scheldt (Fig. 9h) between 1951 and 1998. Similar conclusions apply for both DIN (Fig. 9e) and PO_4 (Fig. 9f) river loads but DIN river loads have a larger influence on the patterns of variation (with lower R for DIN than PO_4), while PO_4 river loads modulate the magnitude of the variability (with lower standard deviation for PO_4 than for N sensitivity results).

Discussion

Global vs. regional response of coastal seas to increased human pressure

Increase of anthropogenic pressures (increasing atmospheric CO_2, increasing population density and socio-economic development) on coastal waters can lead to a modification of their status as sink or source for atmospheric CO_2. The extent to which these activities modify the ability of coastal areas to absorb atmospheric CO_2 and more generally the role of the coastal zone in the global carbon cycle is difficult to appraise because of the nonlinearity of the involved processes and the diversity of coastal seas. Some global modelling approaches have explored the impact of increased nutrient and carbon loads on the heterotrophic or autotrophic status (Ver *et al*., 1999; Rabouille *et al*., 2001) and the direction of the air–sea CO_2 exchanges (Andersson & Mackenzie, 2004; Mackenzie *et al*., 2004) over the past 300 years. However, these studies do not consider the coastal zone ecosystem diversity and the variations of local

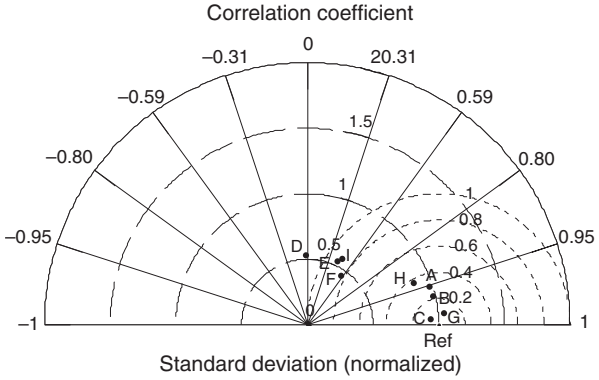

Fig. 9 Normalized Taylor diagram for 1951–1998 annual air–sea CO_2 fluxes computed using real (Ref) or 1951 values for sea surface temperature (A), wind speed (B), atmospheric CO_2 (C) and carbon and nutrient loads for the Seine (I), for the Scheldt (H) or both (D) and separately organic carbon (G), dissolved inorganic nitrogen (DIN) (E) and PO_4 (F) loads for the Seine and the Scheldt. The reference simulation is positioned on the abscissa. The position of each of the other symbols depicts its correspondence with the reference results (the closer to the 'Ref', the better is the correspondence). Its radial distance from origin depicts the normalized standard deviation of the model scenario (a value of 1 indicates similar variability); its distance from the 'Ref' represents the normalized root mean square difference (quantified by dotted circles around the reference); and its azimuthal position corresponds to its correlation with the reference simulation.

anthropogenic pressure. At a global scale, anthropogenic pressure mainly represents the expected evolution for emergent countries which is not representative of the environmental policies actually implemented in watersheds of developed countries. Consequently, although these studies give an average overview of the coastal zone response to the worldwide anthropogenic pressure over the last centuries, they fail to describe the status of a specific coastal ecosystem, in particular if nutrient reduction measures are taken to reduce eutrophication.

R-MIRO-CO_2 is, to our knowledge, the first coupled river–coastal sea model making the link between human activity modifications on the watershed and the status of the coastal zone as sink or source for atmospheric CO_2. Such a tool allows one to assess how the CO_2 sink or source role of the coastal zone has changed in response to changing human activities on the watershed in the past and how it might change in the future.

In this paper, the BCZ was used as a test area to simulate the 1951–1998 evolution of annual NEP and air–sea CO_2 fluxes making use of the MIRO-CO_2 model constrained by reconstructed sea surface temperature, wind speed, atmospheric CO_2 and RIVERSTRAHLER carbon and nutrient river loads. The R-MIRO-CO_2 results show important variability of the air–sea CO_2 fluxes in the BCZ which alternately acts as a source or a sink for atmospheric CO_2 (Fig. 5b). In agreement with the global analysis of Andersson & Mackenzie (2004), a CO_2 source is predicted from the 1950s to the late 1960s when human activities on the watershed and inorganic nutrient loads from rivers to the coastal area were the lowest for the simulation period (Fig. 3). The direction of the CO_2 flux is reversed during the early 1970s and until the mid-1990s. In the late 1990s, our model predicts again a source for atmospheric CO_2 that is comparable with the field-based estimates in the BCZ during that period (Borges & Frankignoulle, 2002; Schiettecatte *et al*., 2006) but differs from the global analysis of Andersson & Mackenzie (2004). The latter suggests a reversal from a source of CO_2 to a sink of CO_2 around 2000 and an increase of the CO_2 sink throughout the 21st century. One of the main difference between the global simulation of Andersson & Mackenzie (2004) and our study is due to the projections of nutrient loads which are assumed to increase exponentially in the global scenario due to emerging economies and fast population growth (Africa, South America and mainly Asia), but to decrease for the BCZ where nutrient and organic carbon delivery reduction policies have been implemented since the 1980s although they have mainly affected the PO_4 river loads.

Contribution of biological activities to annual air–sea CO_2 fluxes

While Mackenzie *et al*. (2004) point to both increased anthropogenic CO_2 emissions to the atmosphere and increasing nutrient river inputs as key players in the reversal of the air–sea CO_2 flux in the global coastal zone, our model sensitivity analysis suggests that inorganic nutrients discharged by rivers are the main drivers of the long-term evolution of annual NEP and air–sea CO_2 fluxes in the BCZ. Increasing atmospheric CO_2 enhances the CO_2 sink in the BCZ but the magnitude of this enhancement is negligible compared with the effect of increased nutrient loads. The obtained different sensitivity to increasing atmospheric CO_2 is related to the difference in model configurations. R-MIRO-CO_2 explicitly computes the exchange of CO_2 with the atmosphere based on the air–sea gradient of pCO_2 and the gas transfer velocity resulting that the water column tracks the increase of atmospheric CO_2 and is at equilibrium with anthropogenic CO_2. The simulated interannual variability of air–sea CO_2 fluxes is then related to changes in carbon cycling driven by variations of river nutrient loadings. In the model of Mackenzie *et al*. (2004), the increase of DIC in surface waters due to invasion of anthropogenic CO_2 is computed as a

fraction of the increase of the atmospheric carbon content using the Revelle factor. Such a mathematical approach ultimately yields a sink of CO_2 due to increasing atmospheric CO_2 that is unrealistic as there is ample evidence that ocean surface waters are at equilibrium with anthropogenic CO_2 (Sabine *et al*., 2004) and that in most regions the long-term trend of pCO_2 in surface waters tracks the increase of atmospheric CO_2 (Takahashi *et al*., 2006, 2008).

In spite of the importance of wind speed and sea surface temperature on the interannual variability of annual NEP and air–sea CO_2 fluxes (Gypens *et al*., 2004), the variability of these forcing cannot explain the long-term trend and the reversal of the air–sea CO_2 flux simulated in the BCZ during the 1951–1998 period. The higher impact of river loads compared with temperature on the long-term trend of coastal air–sea CO_2 flux was also suggested by Ver *et al*. (1999) at a global scale. Additional BCZ sensitivity tests on either carbon or nutrient loads point nutrient changes as the key drivers behind the long-term evolution of air–sea CO_2 fluxes. Of course the increase of organic carbon loads stimulates heterotrophic activities and the emission of CO_2 but this effect is counteracted by primary production stimulated by the concomitant increase of nutrient loads.

Four distinct periods can be identified based on the R-MIRO-CO_2 evolution of inorganic nutrient river loads, the auto- or heterotrophic status and the sink/source role for atmospheric CO_2 of the BCZ (Figs 3, 5a and b). These are:

(1) the period of moderate and well-balanced DIN and PO_4 river inputs (1951–1967) when BCZ is net heterotrophic (NEP $< -0.5\,mol\,m^{-2}\,yr^{-1}$) and is a source of CO_2 to the atmosphere (up to $0.5\,mol\,C\,m^{-2}\,yr^{-1}$).
(2) the eutrophication period (1968–1985) when increased DIN and PO_4 loads are stimulating phytoplankton growth resulting in a progressive decrease of net heterotrophy towards low net autotrophy (annual NEP moves from -0.5 to $+0.5\,mol\,m^{-2}$). The simulated shift of nutrient-enriched coastal waters towards increased autotrophy and increased carbon storage agrees with observations (Smith & Mackenzie, 1987; Smith, 1995) and global simulations (Ver *et al*., 1999). As a result, the BCZ becomes a sink for atmospheric CO_2 reaching a maximum in 1985 when nutrient loads are the highest.
(3) the period of decreasing PO_4 river loads (1986–1993) when the ecosystem metabolic status is close to equilibrium (alternation between low levels of net heterotrophy or net autotrophy) and the CO_2 sink magnitude decreases to neutral exchange of CO_2 with the atmosphere in 1993.
(4) the period of severe unbalanced nutrient river loads (1994–1998) when low PO_4 but excess DIN modify ecological processes so that the BCZ is again net heterotrophic (NEP $< -0.5\,mol\,m^{-2}\,yr^{-1}$) at the end of the period and switches back to an annual source of CO_2 to the atmosphere.

It is generally admitted that net autotrophy induces decreased water pCO_2, and conversely, net heterotrophy corresponds to increase water pCO_2 (e.g. Borges *et al*., 2006). In spite of a significant correlation between R-MIRO-CO_2 annual NEP and air–sea CO_2 flux ($r^2 = 0.72$, $P < 0.001$) over the simulated period, some discrepancies between the heterotrophy/autotrophy status and the CO_2 source/sink in the BCZ are visible from 1968 to 1993 ($r^2 = 0.25$, $P < 0.0001$; Fig. 5).

The 'vegetative period' in the BCZ is characterized by a succession of diatom and *Phaeocystis* blooms (i.e. spring diatoms, *Phaeocystis* colonies and summer diatoms) and their relative contribution to the total primary production shows important variability between 1951 and 1998 (Lancelot *et al*., 2007). Figure 10 compares the seasonal evolution of R-MIRO-CO_2 gross primary production, ecosystem respiration (pelagic and benthic compartments) and air–sea CO_2 flux estimated for 4 typical years (1952, 1980, 1989 and 1994). Clearly, the seasonal evolution is characterized by two periods: a 'winter period' when biological activity is minimal and the air–sea CO_2 exchanges are modulated by river inputs of carbon and seawater temperature (Gypens *et al*., 2004; Fig. 10) and a 'vegetative period', when biological activity controls the magnitude and the direction of the air–sea CO_2 flux (Gypens *et al*., 2004) which alternately acts as a sink or a source for atmospheric CO_2 in response to the balance between photosynthetic and respiration activities (Fig. 10).

Table 2 compares, for the four characteristic periods previously defined, the R-MIRO-CO_2 NEP and air–sea CO_2 fluxes integrated over the winter and vegetative periods. The 'vegetative period' is defined as the period between Julian days 60 and 260 while the 'winter period' corresponds to the rest of the yearly cycle. In winter, respiration is dominant over photosynthesis leading to net heterotrophy and results in a CO_2 emission to the atmosphere (Fig. 10, Table 2). The vegetative period is always net autotrophic but the calculated NEP values vary significantly as well as the corresponding air–sea CO_2 flux which can be either >0 (source) or <0 (sink, Table 2). Over the 1951–1998 simulated period, winter net heterotrophy represents $>50\%$ of annual NEP, while the contribution of corresponding CO_2 source to annual air–sea CO_2 flux is more variable (20–95% of annual flux) being generally $<40\%$ during the 1970s and 1980s. These different contributions of

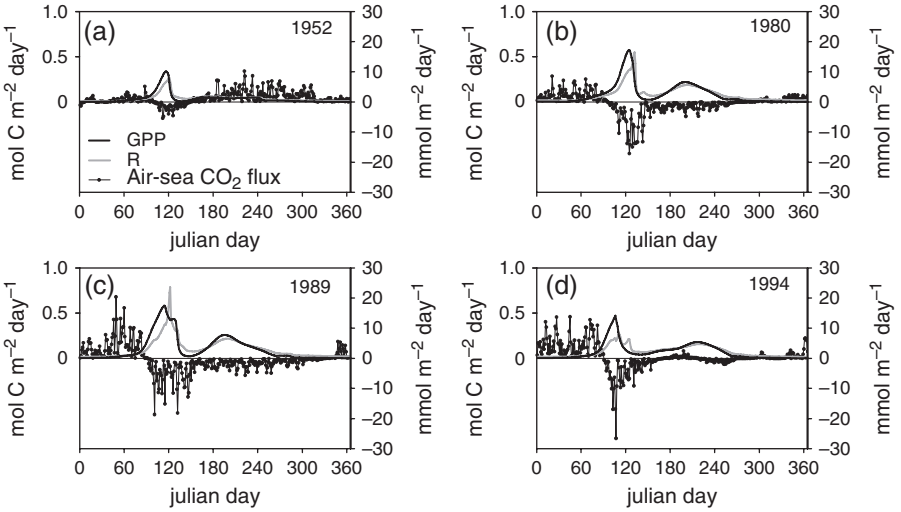

Fig. 10 Seasonal evolution of gross primary production (GPP), ecosystem respiration (*R* in pelagic and benthic compartments) and air–sea CO_2 flux simulated for 1952 (a), 1980 (b), 1989 (c) and 1994 (d).

Table 2 The net ecosystem production (NEP) and air–sea CO_2 fluxes computed by R-MIRO-CO_2 in the Belgian coastal zone (BCZ) integrated for the 'vegetative period' [divided in 'spring period' (Julian days 60–170) and 'summer period' (Julian days 170–260), respectively, left and right term in parentheses] and the 'winter period' (the rest of the yearly cycle)

		NEP		Air–sea CO_2 fluxes	
Period		Vegetative period (spring; summer)	Winter period	Vegetative period (spring; summer)	Winter period
1951–1967	Low nutrient inputs	0.5 (1.2; −0.7)	−1.5	0.2 (−0.1; 0.3)	0.3
1968–1985	Increased nutrient inputs	2.2 (2.1; 0.1)	−2.5	−0.4 (−0.3; −0.1)	0.3
1986–1993	Sustained elevated nutrient inputs	3.1 (2.8; 0.3)	−3.1	−0.7 (−0.5; −0.2)	0.5
1994–1998	Decrease of PO_4 river inputs	1.6 (1.8; −0.2)	−2.4	−0.3 (−0.3; 0.0)	0.4

Integrated fluxes expressed in mmol m^{-2} period^{-1} are averaged for the four characteristic periods identified from the river inorganic nutrient loads.

winter NEP and air–sea CO_2 fluxes to the annual values can explain that, in spite of an annual net heterotrophic status, the BCZ acts as a CO_2 sink during the period 1968–1993 (Fig. 5b).

To better understand the contribution of the vegetative period to carbon fluxes, we divided it in two periods: spring (Julian days 60–170) and summer (Julian days 170–260). The corresponding integrated NEP and air–sea CO_2 fluxes are reported in Table 2. An increased net autotrophic status is simulated during the 'spring vegetative period', mainly attributed to the *Phaeocystis* bloom (not shown) which escapes grazing (Lancelot *et al*., 2005) and accumulates in the water column, and explains the important but transient CO_2 sink (Fig. 10, Table 2). During the 'summer vegetative period' diatoms represent 90% of the summer primary production and the BCZ alternates between net heterotrophy and CO_2 source (1951–1967) and net autotrophy and CO_2 sink (1968–1993) (Table 2). From 1951 to 1967, when inorganic nutrient river loads are low, summer diatom production is moderate and remineralization exceeds photosynthesis (NEP <0) leading to a CO_2 source (Fig. 10a). With the increase of nutrient loads in the early 1970s, summer diatom production largely increases (Lancelot *et al*., 2007) and diatom biomass exceeds the grazing capacity of zooplankton leading to a biomass accumulation in the water column (Fig. 10b and c). Production is in excess compared with organic matter mineralization (NEP >0), and a CO_2 sink is predicted between 1974 and 1993 (Table 2). During the 1990s, summer diatom production (Fig. 10d) decreases in response to the reduction of PO_4 river loads, and the BCZ becomes net heterotrophic and releases CO_2 to the atmosphere. In spite of a weak contribution to annual NEP (but not in terms of gross primary production), the summer diatom bloom is responsible

for the long-term trend of annual air–sea CO_2 fluxes in the BCZ due to the longer water residence time in summer, in addition to the contribution to NEP from the *Phaeocystis* bloom.

Nutrient river loads vs. annual air–sea CO_2 fluxes

Increased human activities on land and concomitant increase of DIN and PO_4 inputs have markedly changed NEP and air–sea CO_2 fluxes in the coastal zone. Our regional model study in the BCZ suggests that this ecosystem shifted from a source to a sink of atmospheric CO_2 due to increased nutrient loads during the 1970s and 1980s but switched back to a CO_2 source in the late 1990s responding to the decreased PO_4 loads. The global analysis of Ver *et al*. (1999) and other related studies suggest a global sustained increase in primary production over the late 21st century and a corresponding monotonic increase in the CO_2 sink in the coastal zone. This discrepancy with our model simulations is explained by the strong change in N : P ratio (>25) of the nutrient loads to the BCZ caused by nutrient reduction policies that were more successful for PO_4 than for DIN.

In conclusion, elevated and well-balanced nutrient loads (compared with nutrient requirement of coastal phytoplankton) stimulate primary production and increase the CO_2 uptake capacity of the BCZ. Low or unbalanced (high N : P ratio) inorganic nutrient inputs limit coastal primary production and the BCZ acts as a source for atmospheric CO_2.

The importance of nutrient ratio and phytoplankton growth limitation on air–sea CO_2 flux in coastal area was also pointed by da Cunha *et al*. (2007), but in their global simulation, only N and Si (and Fe) were considered limiting or co-limiting for phytoplankton growth. Our model results point that in eutrophied areas where nutrient reduction measures have been applied, PO_4 can be the limiting inorganic nutrient (and to a variable degree as a function of the considered phytoplankton community) due to changes in DIN : PO_4 ratios. To correctly simulate long-term changes in primary production and air–sea CO_2 fluxes, limitation or co-limitation by PO_4 has to be included.

Concluding remark

Our results highlight the important but so far neglected coupling between nutrient regulation and mitigation of the emission of greenhouse gases that must be accounted jointly in management policies. We also show that the link between nutrient delivery to the coastal zone and carbon sequestration is complex. Sustained long-term monitoring of key variables (CO_2, inorganic nutrients, phytoplankton composition, etc.) is then required to further unravel and constrain this link and to refine model tools to predict the future evolution of the biogeochemical functioning of the coastal zone and help decision makers and managers.

Acknowledgements

The present work is a contribution to the AMORE (Advanced MOdeling and Research on Eutrophication) project funded by Belgian Science Policy (contract nos. EV-11-19 and SD/NS/03A), to the FP6 European Integrated Project CARBOOCEAN [contract no. 511176 (GOCE)], to the TIMOTHY project (P6/13) funded by the Interuniversity Attraction Poles Programme – Belgian State – Belgian Science Policy, to SOLAS and to COST 735. A. V. B. is an FNRS research associate, N. G. is an FNRS postdoctoral researcher. We acknowledge Fabian Lenartz for help in implementing the Taylor diagram Matlab scripts, Gwenaël Abril for DIC and TA data in the Seine river, and David Smith (Editor), Rachel Knepp (Associate Editor) and two anonymous reviewers for constructive comments on a previous version of the manuscript.

References

Andersson AJ, Mackenzie FT (2004) Shallow-water oceans: a source or sink of atmospheric CO_2? *Frontiers in Ecology and the Environment*, **2**, 348–353.

Billen G, Garnier J, Ficht A, Cun C (2001) Modeling the response of water quality in the Seine river estuary to human activity in its watershed over the last 50 years. *Estuaries*, **24**, 977–993.

Billen G, Garnier J, Hanset P (1994) Modelling phytoplankton development in whole drainage networks: the RIVERSTRAHLER model applied to the Seine river system. *Hydrobiologia*, **289**, 119–137.

Billen G, Garnier J, Rousseau V (2005) Nutrient fluxes and water quality in the drainage network of the Scheldt basin over the last 50 years. *Hydrobiologia*, **540**, 47–67.

Billen G, Servais P, Wargnies S (1991) *Modélisation du transport des polluants par l'Estuaire de l'Escaut*. Cas du Phosphore. Etude réalisée pour le compte de l'Unité de Gestion du Modèle Mathématique de la Mer du Nord et de l'Estuaire de l'Escaut. Ref BH/90/37, Rapport d'avancement, 33 pp, Brussel, Belgium.

Borges AV (2005) Do we have enough pieces of the jigsaw to integrate CO_2 fluxes in the Coastal Ocean? *Estuaries*, **28**, 3–27.

Borges AV, Delille B, Frankignoulle M (2005) Budgeting sinks and sources of CO_2 in the coastal ocean: diversity of ecosystems counts. *Geophysical Research Letters*, **32**, L14601, doi: 10.1029/2005GL023053.

Borges AV, Frankignoulle M (1999) Daily and seasonal variations of the partial pressure of CO_2 in the surface seawater along Belgian and southern Dutch coastal areas. *Journal of Marine Systems*, **19**, 251–266.

Borges AV, Frankignoulle M (2002) Distribution and air–water exchange of carbon dioxide in the Scheldt plume off the Belgian coast. *Biogeochemistry*, **59**, 41–67.

Borges AV, Frankignoulle M (2003) Distribution of surface carbon dioxide and air–sea exchange in the English Channel and

adjacent areas. *Journal of Geophysical Research*, **108**, 3140, doi: 10.1029/2000JC000571.

Borges AV, Schiettecatte L-S, Abril G, Delille B, Gazeau F (2006) Carbon dioxide in European coastal waters. *Estuarine, Coastal and Shelf Science*, **70**, 375–387.

Cai W-J, Dai MH, Wang YC (2006) Air–sea exchange of carbon dioxide in ocean margins: a province-based synthesis. *Geophysical Research Letters*, **33**, L12603, doi: 10.1029/2006GL026219.

Cai W-J, Guo X, Chen CTA *et al*. (2008) A comparative overview of weathering intensity and HCO_3^{2-} flux in the world's major rivers with emphasis on the Changjiang, Huanghe, Zhujiang (Pearl) and Mississippi Rivers. *Continental Shelf Research*, **28**, 1538–1549.

Chen CTA, Borges AV (2008) Reconciling opposing views on carbon cycling in the coastal ocean: continental shelves as sinks and near-shore ecosystems as sources of atmospheric CO_2. *Deep-Sea Research, Part II*, in press.

Chen CTA, Liu KK, Macdonald R (2003) Continental margin exchanges. In: *Ocean Biogeochemistry: The Role of the Ocean Carbon Cycle in Global Change* (ed Fasham MJR), pp. 53–97. Springer-Verlag, Berlin, Germany.

Cloern JE (2001) Our evolving conceptual model of the coastal eutrophication problem. *Marine Ecology Progress Series*, **210**, 223–253.

Cohen JE, Small C, Mellinger A, Gallup J, Sachs J (1997) Estimates of coastal populations. *Science*, **278**, 1211–1212.

da Cunha LC, Buitenhuis ET, Le Quéré C, Giraud X, Ludwig W (2007) Potential impact of changes in river nutrient supply on global ocean biogeochemistry. *Global Biogeochemical Cycles*, **21**, GB4007, doi: 10.1029/2006GB002718.

Dickson AG (1990) Thermodynamics of the dissociation of boric acid in synthetic sea water from 273.15 to 298.15 K. *Deep-Sea Research, Part A*, **37**, 755–766.

Dickson AG, Goyet C (eds) (1994) *Handbook of Methods for the Analysis of the Various Parameters of the Carbon Dioxide System of Sea Water* (2nd edn). ORNL/CDIAC-74, US Department of Energy (DOE, 1994), 36 pp.

Frankignoulle M, Abril G, Borges AV *et al*. (1998) Carbon dioxide emission from European estuaries. *Science*, **282**, 434–436.

Frankignoulle M, Borges AV (2001) Direct and indirect pCO_2 measurements in a wide range of pCO_2 and salinity values (the Scheldt estuary). *Aquatic Geochemistry*, **7**, 267–273, doi:10.1023/A:1015251010481.

Frankignoulle M, Bourge I, Canon C, Dauby P (1996) Distribution of surface seawater partial CO_2 pressure in the English Channel and in the Southern Bight of the North Sea. *Continental Shelf Research*, **16**, 381–395.

Garnier J, Billen G, Coste M (1995) Seasonal succession of diatoms and chlorophyecae in the drainage network of the River Seine: observations and modelling. *Limnology and Oceanography*, **40**, 750–765.

Garnier J, Billen G, Hannon E, Fonbonne S, Videnina Y, Soulie M (2002) Modeling transfer and retention of nutrients in the drainage network of the Danube River. *Estuarine, Coastal and Shelf Science*, **54**, 285–308.

Garnier J, Billen G, Palfner L (1999) Understanding the oxygen budget and related ecological processes in the river Mosel: the RIVERSTRAHLER approach. *Hydrobiologia*, **410**, 151–166.

Gattuso JP, Frankignoulle M, Wollast R (1998) Carbon and carbonate metabolism in coastal aquatic ecosystems. *Annual Review of Ecology and Systematics*, **29**, 405–434.

Gypens N, Lacroix G, Lancelot C (2007) Causes of variability in diatom and Phaeocystis blooms in Belgian coastal waters between 1989 and 2003: a model study. *Journal of Sea Research*, **57**, 19–35.

Gypens N, Lancelot C, Borges AV (2004) Carbon dynamics and CO_2 air–sea exchanges in the eutrophied coastal waters of the Southern Bight of the North Sea: a modelling study. *Biogeosciences*, **1**, 147–157.

Hannon E, Boyd PW, Silvoso M, Lancelot C (2001) Modelling the bloom evolution and carbon flows during SOIREE: implications for future in situ iron-experiments in the Southern Ocean. *Deep-Sea Research, Part II*, **48**, 2745–2773.

Heip C, Goosen NK, Herman PMJ, Kromkamp J, Middelburg JJ, Soetaert K (1995) Production and consumption of biological particles in temperate tidal estuaries. *Oceanography and Marine Biology: An Annual Review*, **33**, 1–149.

Howarth RW, Marino R (2006) Nitrogen as the limiting nutrient for eutrophication in coastal marine ecosystems: evolving views over three decades. *Limnology and Oceanography*, **51**, 364–376.

Kaul L, Froelich P (1984) Modelling estuarine nutrient biogeochemistry in a simple system. *Geochimica et Cosmochimica Acta*, **48**, 1417–1433.

Kemp WM, Smith EM, Marvin-DiPasqual M, Boynton WR (1997) Organic carbon-balance and net ecosystem metabolism in Chesapeake Bay. *Marine Ecology Progress Series*, **150**, 229–248.

Lancelot C (1995) The mucilage phenomenon in the continental coastal waters of the North Sea. *The Science of the Total Environment*, **165**, 83–102.

Lancelot C, Gypens N, Billen G, Garnier J, Roubeix V (2007) Testing an integrated river–ocean mathematical tool for linking marine eutrophication to land use: the Phaeocystis-dominated Belgian coastal zone (Southern North Sea) over the past 50 years. *Journal of Marine Systems*, **64**, 216–228.

Lancelot C, Spitz Y, Gypens N *et al*. (2005) Modelling diatom and Phaeocystis blooms and nutrient cycles in the Southern Bight of the North Sea: the MIRO model. *Marine Ecology Progress Series*, **289**, 63–78.

Ludwig W, Amiotte-Suchet P, Probst JL (1996) River discharges of carbon to the world's oceans: determining local inputs of alkalinity and dissolved and particulate organic carbon. C.R. Academy of Science, Paris, t. 323, Serie II a, pp. 1007–1014.

Mackenzie FT, Lerman A, Andersson AJ (2004) Past and present of sediment and carbon biogeochemical cycling models. *Biogeosciences*, **1**, 11–32.

Mackenzie FT, Ver LM, Lerman A (2002) Century-scale nitrogen and phosphorus controls of the carbon cycle. *Chemical Geology*, **190**, 13–32.

Mehrbach C, Culberson CH, Hawley JE, Pytkowicz RM (1973) Measurements of the apparent dissociation constants of carbonic acid in seawater at atmospheric pressure. *Limnology and Oceanography*, **18**, 897–907.

Middelburg JJ, Duarte CM, Gattuso JP (2005) Respiration in coastal benthic communities. In: *Respiration in Aquatic Ecosystems* (eds

del Giorgio PA, Williams PJLB), pp. 206–224. Oxford University Press, Oxford.

Middelburg JJ, Soetaert K (2004) The role of sediments in shelf ecosystem dynamics. In: *The Global Coastal Ocean: Multiscale Interdisciplinary Processes* (eds Robinson AR, Brink K), pp. 353–374. Harvard University Press, Cambridge.

Nightingale PD, Malin G, Law CS *et al*. (2000) In situ evaluation of air–sea gas exchange parameterizations using novel conservative and volatile tracers. *Global Biogeochemical Cycles*, **14**, 373–387.

Nixon SW (1995) Coastal marine eutrophication: a definition, social causes, and future concerns. *Ophelia*, **41**, 199–219.

Officer CB, Ryther JH (1980) The possible importance of silicon in marine eutrophication. *Marine Ecology Progress Series*, **3**, 83–91.

Rabouille C, Mackenzie FT, Ver LM (2001) Influence of the human perturbation on car – carbon, nitrogen, and oxygen biogeochemical cycles in the global coastal ocean. *Geochimica et Cosmochimica Acta*, **65**, 3615–3639.

Sabine CL, Feely RA, Key RM *et al*. (2004) The oceanic sink for anthropogenic CO_2. *Science*, **305**, 367–371.

Schiettecatte L-S, Gazeau F, Van der Zee C, Brion N, Borges AV (2006) Time series of the partial pressure of carbon dioxide (2001–2004) and preliminary inorganic carbon budget in the Scheldt plume (Belgian coast waters). *Geochemistry, Geophysics, Geosystems (G3)*, **7**, Q06009, doi: 10.1029/2005GC001161.

Smith SV (1995) Net carbon metabolism of oceanic margins and estuaries. In: *Biotic Feedbacks in the Global Climatic System: Will the Warming Feed the Warming?* (eds Woodwell GM, Mackenzie FT), pp. 251–262. Oxford University Press, Oxford, UK.

Smith SV, Hollibaugh JT (1993) Coastal metabolism and the oceanic carbon balance. *Reviews of Geophysics*, **31**, 75–89.

Smith SV, Mackenzie FT (1987) The ocean as a net heterotrophic system: implications from the carbon biogeochemical cycle. *Global Biogeochemical Cycles*, **1**, 187–198.

Smith SV, Swaney DP, Talaue-Mcmanus L *et al*. (2003) Humans, hydrology, and the distribution of inorganic nutrient loading to the ocean. *Bioscience*, **53**, 235–245.

Soetaert K, Middelburg JJ, Heip C, Meire P, Van Damme S, Maris T (2006) Long-term change in dissolved inorganic nutrients in the heterotrophic Scheldt estuary (Belgium, the Netherlands). *Limnology and Oceanography*, **51**, 409–423.

Takahashi T, Sutherland SC, Feely RA, Wanninkhof R (2006) Decadal change of the surface water pCO_2 in the North Pacific: a synthesis of 35 years of observations. *Journal of Geophysical Research*, **111**, C07S05, doi: 10.1029/2005JC003074.

Takahashi T, Sutherland CS, Wanninkhof R *et al*. (2008) Climatological mean and decadal change in surface ocean pCO_2, and net sea–air CO_2 flux over the global oceans. *Deep-Sea Research, Part II*, in press.

Taylor KE (2001) Summarizing multiple aspects of model performance in a single diagram. *Journal of Geophysical Research*, **106**, 7183–7192.

Thomas H, Bozec Y, Elkalay K, de Baar HJW (2004) Enhanced open ocean storage of CO_2 from shelf sea pumping. *Science*, **304**, 1005–1008.

Van Beusekom JEE, de Jonge VNN (2002) Long-term changes in Wadden-Sea nutrient cycles: importance of organic matter import from the North Sea. *Hydrobiologia*, **475/476**, 185–194.

Ver LM, Mackenzie FT, Lerman A (1999) Carbon cycle in the coastal zone: effects of global perturbations and changes in the past three centuries. *Chemical Geology*, **159**, 283–304.

Vitousek PM, Aber JD, Howarth RW *et al*. (1997) Human alteration of the global nitrogen cycle: sources and consequences. *Ecological Applications*, **7**, 737–750.

Weiss RF (1974) Carbon dioxide in water and seawater: the solubility of a non-ideal gas. *Marine Chemistry*, **2**, 203–215.

Wollast R (1998) Evaluation and comparison of the global carbon cycle in the coastal zone and in the open ocean. In: *The Sea: The Global Coastal Ocean, Processes and Methods* (eds Brink KH, Robinson AR), pp. 213–252. John Wiley and Sons Inc., New York, NY.

